การวิเคราะห์โดเมนเวลาขณะเกิดผลตอบสนองอิมพัลส์ของแท่งอิเล็กโตรดต่อลงดินในชั้นใต้ดิน 2 ชั้นที่สภาวะทรานเชี้ยนต์โดยวิธี Boundary Finite Element Method

ชำนิ ใจประดิษฐ์ธรรม*

รองศาสตราจารย์ สาขาวิชาวิศวกรรมไฟฟ้า คณะวิศวกรรมศาสตร์ มหาวิทยาลัยเกษมบัณฑิต

บทคัดย่อ

บทความวิจัยนี้นำเสนอถึงการวิเคราะห์โดเมนเวลาในขณะเกิดผลตอบสนองอิมพัลส์ของแท่งอิเล็กโตรดต่อลงดินเมื่อพิจารณาโครงสร้างชั้นใต้ดิน 2 ชั้นของระบบต่อลงดินในสภาวะช่วงทรานเชี้ยนต์ ซึ่งมีการประยุกต์โดยใช้วิธีการจำกัดขอบเขตองค์ประกอบ (The Boundary Finite Element Method: BFEM) ในงานวิจัยนี้นำเสนอวิธีใหม่เพื่อคำนวณผลตอบสนองอิมพัลส์ฟ้าผ่าที่เกิดขึ้น ซึ่งเป็นองค์ประกอบพื้นฐานในการวิเคราะห์ระบบต่อลงดิน ได้แก่ แท่งอิเล็กโตรดต่อลงดิน ความต้านทานดิน โดเมนเวลา ลักษณะกระแสลำฟ้าผ่าที่ไหลลงสู่ดินซึ่งเทียบกับฟังก์ชันเวลา โดยใช้สมการคณิตศาสตร์ในการวิเคราะห์เพื่อแสดงให้เห็นว่าในระบบต่อลงดินทำให้เกิดกระแสไฟฟ้าและแรงดันไฟฟ้าแผ่กระจายไหลผ่านแท่งอิเล็กโตรดลงสู่ดิน ผลการเกิดไอออไนเซชันของดินสามารถนำไปใช้อธิบายเหตุผล วิธีการ BFEM ที่นำเสนอนี้จะแสดงผลการจำลองรูปคลื่นกระแสไฟฟ้าและแรงดันไฟฟ้าแผ่กระจายไหลผ่านแท่งอิเล็กโตรดเทียบกับเวลาโดยใช้โปรแกรม MATLAB เพื่อคำนึงถึงความปลอดภัยในการติดตั้งระบบต่อลงดินของสถานีไฟฟ้าย่อยแรงสูง และมีความเชื่อมั่นในความปลอดภัยของคนจากแรงดันสัมผัสและแรงดันช่วงก้าว

คำสำคัญ: แท่งอิเล็กโตรดต่อลงดิน ผลตอบสนองฟ้าผ่า ชั้นดิน 2 ชั้น แรงดันเกินทรานเชี้ยนต์

Time Domain Analysis Regarding Transient Performance of a Grounding System Installed in a Two-layer Soil Structure Using the Boundary Finite Element Method

Chamni Jaipradidtham*

Associate Professor, Department of Electrical Engineering, Faculty of Engineering, Kasem Bundit University, Bangkok, Thailand

* Corresponding Author, Tel. 0-2320-6930, E-mail: j_chamni@hotmail.com

Abstract

    In this study, transient responses of the grounding electrode installed in a 2-layer soil structure in time domain schemes were analyzed based on the boundary *finite element method* (BFEM). A new methodology to estimate lightning impulse responses was presented whereas related components, i.e. impulse-current dispersal of grounding electrode, soil resistivity, time-domain responses and lightning strike models in exponential time functions were taken into account. Mathematical formulas were applied to determine current and voltage distribution along the electrode while soil ionization phenomena could be used for further description. Time domain analysis of the grounding electrode impulse was carried out based on the BFEM. Through MATLAB, the simulations were performed to ensure a safe grounding system for power generation stations coupled with an awareness of step and touch potentials in which personal safety remains a primary concern

Keywords: Grounding Electrode, Lightning Responses, Two-layer Soil Structure, Transient Overvoltage

1. Introductions

Analysis of the grounding systems subjected to lightning impulse current is complicated and the transient impulse response of grounding electrodes results in almost empirical formulation of lightning protection. This paper presents for time domain analysis of a grounding system for transient by applying the BFEM method for the analytical calculation of the behavior of a grounding electrode under transient conditions. Finally, efficient and accurate numerical formulations have been derived from this BFEM method approach. The BFEM method belongs to the second category of methods (i.e., the grounding electrode is treated as an open ended transmission lines or as a series of π-circuits). Telegraphy equations are used and analytical formulae are obtained for current and voltage distributions along the grounding electrode in a two layer soil model. The difference with previous attempts is that no particular assumptions for the energization source or the length of the electrode are required, a linearly increasing current at the start is considered.

In the method proposed in the paper, lightning injection current is modeled as a typical double exponential function. It is shown in Figure 1 that from the infinite series of terms comprising the general solution for voltage and current, a small number of terms is needed to provide results of satisfactory accuracy in most practical cases. The results from the analytical calculation of the lightning impulse response of horizontal grounding electrode are presented. The impulse impedance and defined as the ratio of the instantaneous potential rise at the injection point to the energization current and the impulse coefficient, defined the impulse impedance to the frequency resistance [1]. The results obtained are validated with
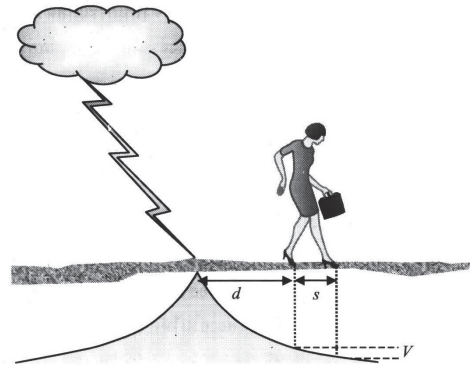

Figure 1 The step voltage critical of the person in grounding system when lightning strikes [1].
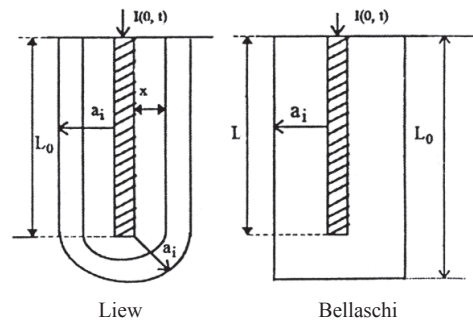

Figure 2 Grounding electrode for a two layered soil ionization model.

experimental data and compared with results obtained from other analytical of the numerical methods are Ritz method, Galerkin method and variational method.

2. Analysis

2.1 Potential Distribution Along the Ground Electrode

Potential distribution along the ground electrode for a two layered soil model. Grounding electrodes are characterized by per unit length series resistance R_e, series inductance L_e; shunt conductance G_e [2]; and shunt capacitance C_e. However, the voltage and current distribution along the electrodes must satisfy the telegraphy equations, as shown in Figure 2 [2].
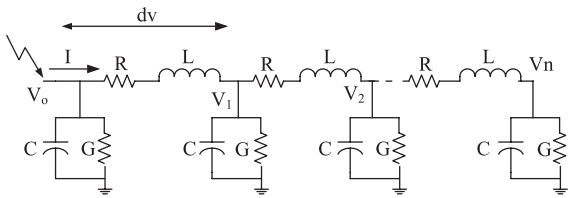
Figure 3 Voltages and currents at lumped elements of the equivalent circuit network.

For the purposes of our analysis grounding electrodes are modeled as a network of series connected π-equivalent circuits with lumped R-L-C elements, where each π-circuit corresponds to a small conductor as shown in Figure 3. In this condition, the equations of telegraphy are expressed through magnetic and electric fluxes as follows:

$$-\frac{\partial V(x,t)}{\partial x} = R_e I(x,t) + L_e \frac{dI(x,t)}{dt} \tag{1}$$

$$-\frac{\partial I(x,t)}{\partial x} = G_e V(x,t) + C_e \frac{dV(x,t)}{dt} \tag{2}$$

The models suppose the ground rod radius is not a function of x shown in equation (1) and (2), where the radius of the ground rod is a function of time [3]. It is obvious that distributed parameters R, L, C and G. Mathematical analysis of this network requires:

1) formulation of the expressions of voltages and currents for the equivalent network of π-circuits;

2) calculation of their limits as the number of π-circuits increases.

The network model of the electrode is equivalent to an open-ended transmission line. The first stage of this calculation involves determination of the voltages and currents V_0 and I at each as shown in Figure 3.

2.2 Boundary Finite Element Numerical Analysis

BFEM numerical approach has been applied to the grounding analysis of a real electrical installation. The grounding system protection is area of 38,000 m². The studied area is a wider superimposed rectangular zone of 300×260 m². The ground potential rise (GPR) considered in this study is 10 kV [3]. The plans of the earthing grid as shown in Figure 4 and Figure 5, the general data (see in Table 1) were obtained from the grounding plans and specifications of the substation. The characteristics of the numerical model that has been used in this example can be found in Table 1.

Table 1 Grounding system: Characteristics and BFEM numerical model [3]

Data	
Number of Electrode	534
Number of Ground Rods	24
Diameter of Electrodes	11.28 mm
Diameter of Ground Rods	15.00 mm
Depth of the Grid	0.75 m
Length of Ground Rods	4 m
Max. Dimensions of Grid	230×195 m²
GPR	10 kV
BFEM Numerical Model	
Type of Element	Linear
Number of Elements	582
Degrees of Freedom	386

Table 2 Grounding system: Obtained for different soil

One Layer Soil Model	
Soil Resistivity	60 Ω - m
Total Current	6.73 kA
Equivalent Resistance	0.149 Ω
Two Layer Soil Model	
Upper Layer Resistivity	200 Ω -m
Lower Layer Resistivity	60 Ω -m
Thickness Upper Layer	1.2 m
Total Current	5.61 kA
Equivalent Resistance	0.178 Ω

In Table 2 compares the numerical results, the equivalent resistance and the total electrical current leaked into the ground of the analysis. Figure 4 and 5, shown the potential distributions on the earth surface when the grounding electrode attains the GPR voltage,
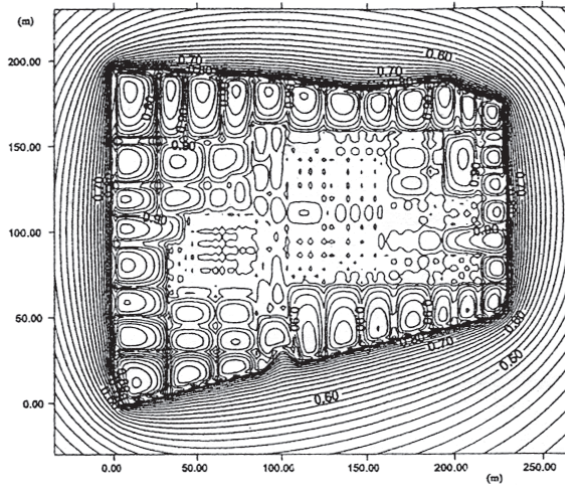
Figure 4 Grounding system: Potential distribution (x10kV) on ground surface obtained with a homogeneous and isotropic soil model: vertical axis and horizontal axis of graph shown the potential distributions width (m).
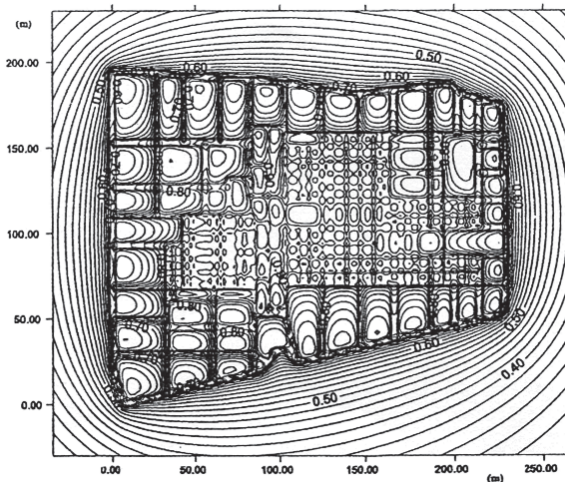

Figure 5 Grounding system: Potential distribution (x10kV) on ground surface obtained with a two layer soil model: vertical axis and horizontal axis of graph shown the potential distributions width (m) on the earth.
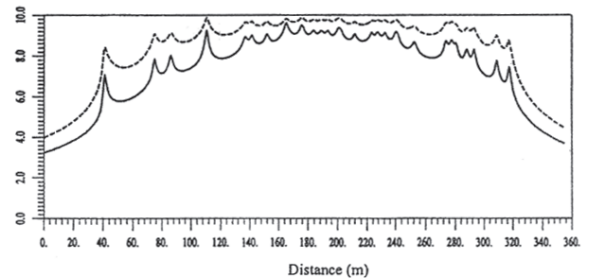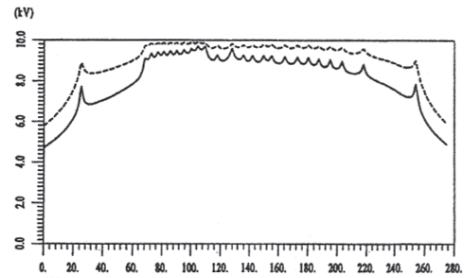

Figure 6 Profiles of potential distribution on the soil earth surface along two lines: vertical axis of graph shown the potential distributions voltage (kV) and horizontal axis of graph the distance (m) of the electrode [4].

obtained by using the homogeneous and isotropic soil model and the proposed two layer soil, remark that the analysis of this grounding system with the two layer soil model is particularly difficult. Because the length of the ground electrode is 4 m and higher than the height of the upper layer is 0.75 m.

It is obvious that both potential distributions. It is known that noticeably different contour drawings do not necessarily correspond to significant differentces between the plotted results as shown in Figure 6, compare the potential profiles computed with the two soil along two different lines on the ground surface.

The Kirchoff's laws for voltages and currents need to be satisfied at any point of the network [4].

$$\lim_{n \to \infty} i_k(t) = I_p(x,t)$$

$$= I_0 \left(\frac{\sinh(\gamma_\alpha(\ell - x))}{\sinh(\gamma_\alpha \ell)} e^{\alpha . t} - \frac{\sinh(\gamma_\beta(\ell - x))}{\sinh(\gamma_\beta \ell)} e^{\beta . t} \right) \quad (3)$$

Telegraphy equations result in voltage distribution as follows:

$$V_p(x,t) = I_0 \left(\frac{-\cosh(\gamma_\alpha(\ell - x))}{\sinh(\gamma_\alpha \ell)} \cdot \frac{\gamma_\alpha}{G_e + \alpha . C_e} e^{\alpha . t} \right.$$
$$- \frac{-\cosh(\gamma_\beta(\ell - x))}{\sinh(\gamma_\beta \ell)} \cdot \frac{\gamma_\beta}{G_e + \beta . C_e} e^{\beta . t} \quad (4)$$
$$\left. + const . e^{-(G_e t / C_e)} \right)$$

Where $\gamma_\alpha = \sqrt{(R_e + \alpha L_e)(G_e + \alpha C_e)}$ and $\gamma_\beta = \sqrt{R_e + \beta L_e)(G_e + \beta C_e)}$.

The above partial solution must be completed by the general solution of the homogeneous differential equation. This is expressed by the following equations for current and voltage, correspondingly:

$$I_h(x,t) = I_o \sum_{k=1}^{\infty} \left\{ C_1(k) . \frac{\sinh(\gamma_{r1(k)}(\ell - x))}{Z_{r1}(k)} . e^{r1(k) . t} \right.$$
$$\left. + C_2(k) . \frac{\sinh(\gamma_{r2(k)}(\ell - x))}{Z_{r2}(k)} . e^{r2(k) . t} \right\}$$
$$(5)$$

$$V_h(x,t) = I_0 \sum_{k=1}^{\infty} \left\{ C_1(k) . \cosh(\gamma_{r1(k)}(\ell - x)) . e^{r1(k) . t} \right.$$
$$+ C_2(k) . \cosh(\gamma_{r2(k)}(\ell - x))$$
$$\left. . e^{r2(k) . t} \right\}$$
$$(6)$$

where

$$r_1(k) = \frac{-R_e C_e \ell^2 - L_e G_e \ell^2 + \Delta}{2L_e C + e}$$

$$r_2(k) = \frac{-R_e C_e \ell^2 - L_e G_e \ell^2 + \Delta}{2L_e C_e}$$

$$\Delta = \sqrt{R_e C_e \ell^2 - L_e G_e \ell^2)^2 - 4L_e C_e \ell^2 - \pi^2 k^2}$$

$$Z_{r1}(k) = \sqrt{\frac{R_e + r_1(k) L_e}{G_e + r_1(k) C_e}}$$

$$Z_{r2}(k) = \sqrt{\frac{R_e + r_2(k) L_e}{G_e + r_2(k) C_e}}$$

$$\gamma_{ri(k)} = \sqrt{(R_e + r_i(k) L_e)(G_e + r_i(k) C_e)}$$

Consequently, current and voltage at any point of the electrode at any time are given by equation (7)

$$I(x,t) = I_h(x,t) + I_p(x,t)$$
$$V(x,t) = V_h(x,t) + V_p(x,t) \quad (7)$$

Expressions (5) and (6) comprise sums of infinite terms, only a few terms are needed, however [5]-[7], to approximate the solution with satisfactory accuracy.

The number of these infinite terms depends on the electrode length, soil resistivity, relative permittivity ε_{r1}, ε_{r2} and the rise time of the injection current. It increases as the length of the electrode increases and as the soil permittivity decreases. It should be noted that accuracy within less than 1% is obtained with only one term when the response of electrode lengths shorter than the "effective length" determined in [8], is calculated. In electrodes longer than the "effective length," however, three terms provide results with an error < 1% in practical cases examined. These terms should be selected from the values $r_{1,2}(k)$. The fact that very few terms are needed in the final expressions (5) and (6) greatly simplifies the method making it

suitable for use in analytical calculations. It should be noted that apart from this simplification, closed form expressions have been used in the main stages of the procedure, which are close to the parameters of the injected double exponential α, β.

All constants of e $C_1(k)$ and $C_2(k)$ in (5) and (6) and in (3) are determined in order to satisfy the initial conditions of propagation of current and voltage traveling waves.

$$I(x, x\sqrt{L_eC_e}) = 0$$
$$V(x, x\sqrt{L_eC_e}) = 0 \qquad (8)$$

or

$$I_h(x, x\sqrt{L_eC_e}) + I_p(x, x\sqrt{L_eC_e}) = 0 \qquad (9)$$

$$V_h(x, x\sqrt{L_eC_e}) + V_p(x, x\sqrt{L_eC_e}) = 0 \qquad (10)$$

It is convenient to use the auxiliary functions:

$$f(k, x) = \sum_{i=1,2} \frac{\sinh(\gamma_{ri(k)}(\ell - x))}{Z_{ri}(k)} \cdot e^{ri(k).x.\sqrt{L_eC_e}}$$

$$g(k, x) = \sum_{i=1,2} \cosh(\gamma_{ri(k)}(\ell - x)) \cdot e^{ri(k).x.\sqrt{L_eC_e}} \quad (11)$$

$C_1(k)$ are set equal to $C_2(k)$, in order to have real values of current $I_h(x, t)$ and $V_h(x, t)$ when the roots $r_i(k)$ are complex, this works well also the roots are real. In the expressions (3)-(6), forward and backward traveling waves can be distinguished for current:

$$I^\pm(x,t) = \frac{\pm e^{\alpha.t \pm \gamma_\alpha(\ell-x)}}{\sinh(\gamma_\alpha \ell)} - \frac{\pm e^{\beta.t \pm \gamma_\beta(\ell-x)}}{\sinh(\gamma_\beta \ell)}$$
$$\pm \sum_{k=1}^{\infty} \left\{ C_1(k). \frac{e^{r_1(k).t \pm \gamma_{r1}(k)(\ell-x)}}{Z_{r1}(k)} \right.$$
$$\left. + C_2(k). \frac{e^{r_2(k).t \pm \gamma_{r2(k)}(\ell-x)}}{Z_{r2}(k)} \right\} \qquad (12)$$

In equation (12), $I^+(x, t)$ is the sum of all forward
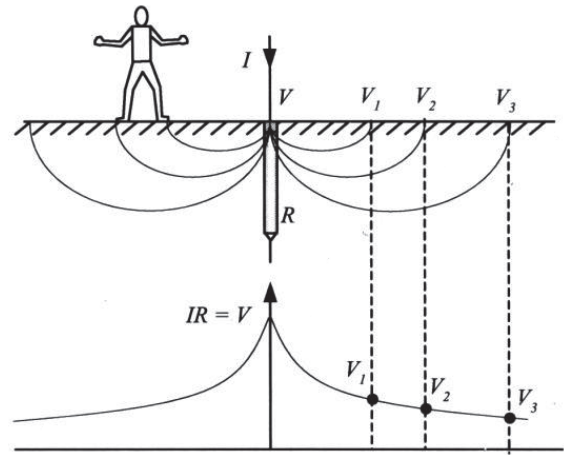

Figure 7 The potential voltage difference between two points on the ground when the ground electrode for a two layered soil, cause the touch voltage and the step voltage [3].

current waves and $I^-(x, t)$ is the sum of all backward waves. When total current at point is given as the sum $I(x, t) = I^+(x, t) + I^-(x, t)$. A similar expression is used for voltage $V(x, t) = V^+(x, t) + V^-(x, t)$.

In this general, it has higher value than the steady state resistance, although a lower value may appear at the first is depending on the electrode characteristics as show in Figure 7.

$$V^\pm(x,t) = \frac{-e^{\alpha.t \pm \gamma_\alpha(\ell-x)}}{\sinh(\gamma_\alpha \ell)} \cdot \frac{\gamma_\alpha}{G_e + \alpha C_e}$$
$$- \frac{-e^{\beta.t \pm \gamma\beta(\ell-x)}}{\sinh(\gamma_\beta \ell)} \cdot \frac{\gamma B}{G_e + \beta C_e}$$
$$- \sum_{k=1}^{\infty} \left\{ C_1(k).e^{r2(k).t \pm \gamma_{r1(k)}(\ell-x)} \right.$$
$$\left. + C_2(k).e^{r2}(k).t \pm \gamma_{r2(k)}(\ell-x) \right\} \qquad (13)$$

Impulse impedance is defined as the ratio of the

transient potential at the injection point to the current.

$$Z(0,t) = \frac{V(0,t)}{I(0,t)} \qquad (14)$$

2.3 Soil Ionization

When large current densities are injected in the electrode, large currents emanate from its surface to the soil. When the critical field strength exceeds a particular value, breakdown of the soil occurs. In this case, the electrode will be surrounded by a cylindrical corona-type discharge pattern [9]-[11], which augments its practical radius and makes the dispersion of the current from its surface to the earth easier. The critical breakdown strength E_{crit} of the surrounding soil can be obtained from the following formula:

$$E_{crit} = 241.\sigma_E^{-0.215} \qquad (15)$$

where E_{crit} is in kilovolts per meter, σ_E is in $(\Omega m)^{-1}$

In the method proposed in this paper, soil ionization can be easily accommodated at a given time t by modification of the ground electrode radius as follows.

1) Current and voltage distribution along the electrode are calculated for given soil characteristics, impulse current, and electrode geometry.

2) The field strength is calculated, leading to a respective change of the conductor radius, if applicable [9]. Modified conductor radius is given from the formula $r = (I_\rho / 2\pi / E_c)$, the values I is the leakage current at a discrete point, ρ is the resistivity of soil, and E_c is the critical electric field intensity value.

3) When current and voltage distributions are calculated for the new radius of the conductor which is changing along the electrode.

4) For the next time, steps 2 and 3 are repeated.

3. The New BFEM Iterative Numerical Algorithm

Figure 8 shows the flowchart of new the proposed algorithm. In this research. It is then used as boundary condition for finite element method resolution of diffusion equation. The new BFEM has the advantage that the potential $V(x, t)$ and the current $I(x, t)$ may be known for any point at a discreet time (time step equals 0.01 μs in the simulation). The transient potential distribution voltage above the surface of the ground corresponds. In the interval corresponding to one step of time in the simulation, these coefficients are taken equal to their value in this time, and viewed as constant. The potential distribution $V(x, t)$ at soil surface is then easily obtained. In Figure 8 gives the algorithm used. Theoretically, the null potential is at infinity. For practical reasons, the domain is limited to a radius of 70 m. This is confirmed by measurements. The transient response of grounding electrodes results in almost empirical formulation of lightning protection method in a two layer soils structure of grounding system.

4. The Simulation Results

Validation of the proposed method is based on experimental data from literature. Test electrode and injection current are described in Table 3. Soil has resistivity 60 Ω-m and permittivity 80. When current injected has low values so soil ionization phenomena can be neglected. Results are plotted in the following Figure 9-12. They are contrasted to experimental data and results obtained from using MATLAB program, and where the electrode is modeled using a series of circuits, similar to the model as shown in Figure 3. It is shown that the results are almost identical to those
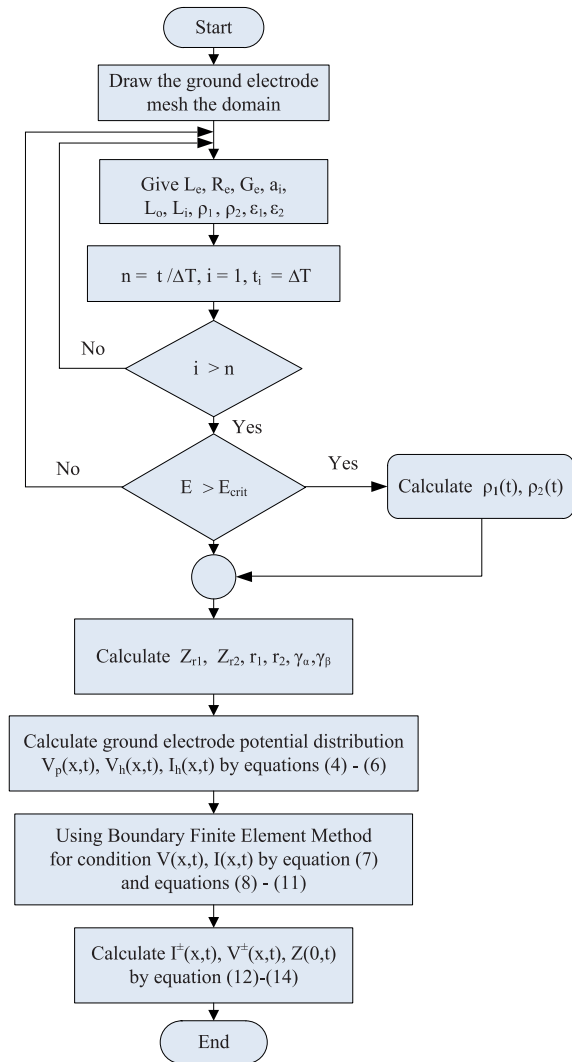
Figure 8 Flowchart of the BFEM iterative numerical algorithm.

Figure 9 Current distribution versus time at various points of a 140 m long electrode buried in high relative permittivity soil (ε_r = 50).

Figure 10 Current distribution versus time at various points of a 140 m long electrode buried in low relative permittivity soil l (ε_r = 1).

from using program and close to experimental ones. The proposed model is applied to the transient analysis of a 140 m long electrode with a radius of 1.5 mm buried in 0.9 m in 300 Ω-m soil. Injection current has a 7/28-μs waveform. Many attempts have therefore been made in the past for the calculation of this transient behavior. They can be divided in two main categories:
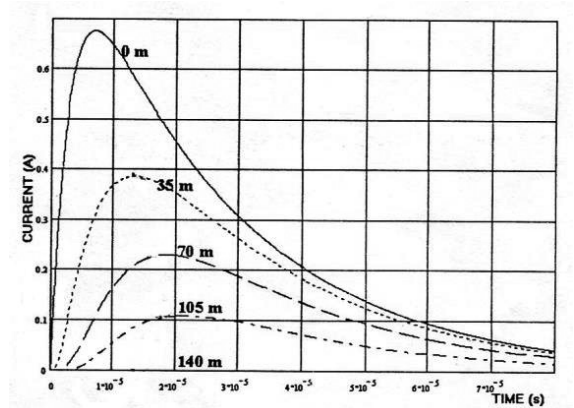
1) those based on frequency domain calculations with subsequent transformation of the solution in time domain using inverse fast Fourier transformation (IFFT) and 2) those based in calculation of the solution directly in the time domain. The current and the voltage values at various points of the electrode are in Figure 9-12. Soil resistivity of the surrounding soil decays in an exponential manner, when ionization occurs.

Figure 11 Voltage distribution versus time at various points of a 140 m long electrode buried in high relative permittivity soil ($\varepsilon_r = 50$).

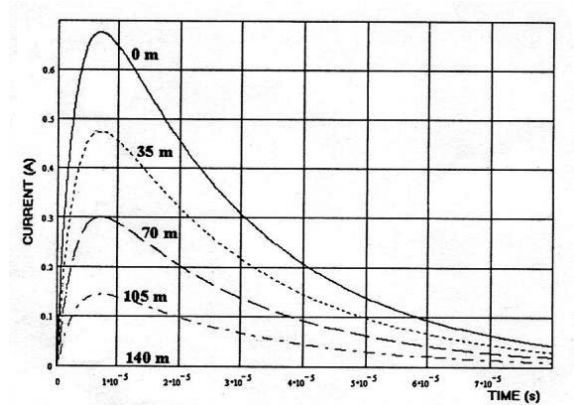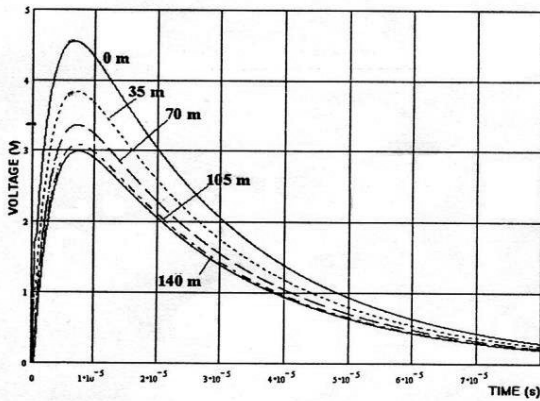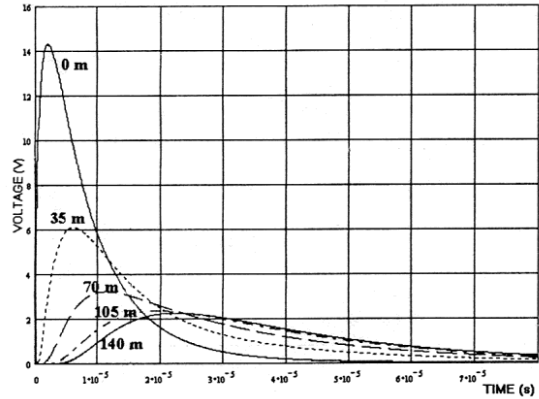**Figure 12** Voltage distribution versus time at various points of a 140 m long electrode buried in low relative permittivity soil ($\varepsilon_r = 1$).

Table 3 Input data for model application

Test Electrode		Injection Current
Length	100 m	$I_{source}(t) = I_0 \cdot (e^{at} - e^{\beta t})$
Diameter	3 mm	$I_0 = 1.55227\,A$
Burial depth	0.60 m	$\alpha = .3640, \beta = -652210$
$\rho_e = 0.25\,E - 6\,\Omega - m$		

It can be observed that currents and voltages at any point of the electrode have almost the same wave shape versus time as the injected current when $\varepsilon_r = 50$ as shown in Figure 9 and 11. When relative permittivity is low, the effect of the capacitive component weakens. In this case, the electrode shows a reactive behavior. This results in faster appearance of the voltage peak at the injection point and distortion of the current waveshape along the electrode.

Maximum current value decrease as the distance form the start increases, until it reaches zero at the electrode end as shown in Figure10. This results in modification of R-L-C parameters of the equivalent ladder network that represents the ground electrode, according to an exponential rule. This is expected from the theory of traveling waves at the open-ended transmission line, since current waves are fully reflected at the end of the electrode, giving a zero total current value at this point.

The ratio of the maximum voltage at any fixed distance x to the maximum voltage V_{max} at the current injection point decreases as the electrode length increases, because the increased length weakens the effect of superposition of reflections at the end.

This is shown in Figure 12 where experimental results and analytical formulae (7), (9), (10) have been contrasted for the calculation of V_x / V_0 ratio for the simulated 140 m long electrode in 300 Ω-m soil. The electrode under consideration is a 8.61 m buried horizontal electrode excited by 22.2 kA impulse current. Voltages and currents have been calculated for the first 30 μs. At the present moment, the study of large installations with two layer soil models still requires an important computing effort. In fact, two layer models can be used in real time and the transient potential distribution voltage above be surface of the

ground corresponds to the transient ground potential rise for homogeneous or heterogeneous soil. It is easy to investigate at distance from the ground rod the transient potential rise does not exceed 1,000 V.

5. Conclusions

In this paper, a new method for the analysis of the transient behavior of grounding electrodes in presented. A boundary element approach for the analysis of substation earthing systems in layered soils has been presented in this paper. Thus, accurate results should be obtained in practical cases with a relatively small computational cost. The proposed BEM technique has been implemented in a computer aided design system developed by the authors for grounding substation design. The proposed approach has been applied to a practical case, and the results obtained by means of both, a single and a two layer soil model, have been compared. The results obtained from comparison method of the current and voltage distribution at various points for time: t = 0.5 × 10^{-5} S and ε_r = 50 as shown in Table 4 and Table 6. The results obtained from comparison method of the current and voltage distribution at various points for time : t = 1.5 × 10^{-5} S and ε_r = 1 as shown in Table 5 and Table 7. Thus, it is characterized by the following advantages.

Table 4 Results obtained from comparison method of the current distribution at various points for time: t = 0.5×10^{-5} S and ε_r = 50

Long Electrode	35 m	70 m	105 m	140 m
BFEM Method	0.47 A	0.29 A	0.14 A	0 A
Ritz Method	0.42 A	0.21 A	0.13 A	0 A
Galerkin Method	0.45 A	0.27 A	0.14 A	0 A
Variational Method	0.44 A	0.25 A	0.11 A	0 A

Table 5 Results obtained from comparison method of the current distribution at various points for time: t = 1.5×10^{-5} S and ε_r = 1

Long Electrode	35 m	70 m	105 m	140 m
BFEM Method	0.39 A	0.22 A	0.11 A	0 A
Ritz Method	0.37 A	0.20 A	0.09 A	0 A
Galerkin Method	0.40 A	0.21 A	0.12 A	0 A
Variational Method	0.36 A	0.19 A	0.11 A	0 A

Table 6 Results obtained from comparison method of the voltage distribution at various points for time: t = 0.5×10^{-5} S and ε_r = 50

Long Electrode	35 m	70 m	105 m	140 m
BFEM Method	3.8 V	3.4 V	3.15 V	3 V
Ritz Method	3.5 V	3.3 V	3.12 V	2.9 V
Galerkin Method	3.4 V	3.3 V	3.11 V	2.7 V
Variational Method	3.6 V	3.2 V	3.13 V	2.9 V

Table 7 Results obtained from comparison method of the voltage distribution at various points for time: t = 1.5×10^{-5} S and ε_r = 1

Long Electrode	35 m	70 m	105 m	140 m
BFEM Method	3.9 V	3.5 V	2.4 V	1.90 V
Ritz Method	3.7 V	3.2 V	2.2 V	1.76 V
Galerkin Method	3.6 V	3.4 V	2.3 V	1.83 V
Variational Method	3.7 V	3.3 V	2.4 V	1.85 V

1) The method is based on closed form solution of the telegraphy equations. The solution is achieved directly in time domain, so any transformation to and from the frequency domain is not required.

2) The proposed method is general (no particular assumptions for the form of the energization source or the length of the electrode are required).

3) Convergence to fifth decimal point is achieved

using only a few terms (up to four) of the infinite series expressing analytically the current and voltage distributions, while the initial conditions are fully satisfied. This simplification simplifies and accelerates calculations of grounding system.

4) Results compare very satisfactorily with field measurements or results from other analytical or numerical methods. A good agreement is also observed in case soil ionization is incorporated in the analysis.

References

[1] IEEE. Std 80-2000, *IEEE Guide for Safety in AC Substation Grounding*, in approved 30 January, 2000.

[2] A. Keshmiri and V.J. Arnautovski, "Frequency dependent and transient impedance of grounding systems: Comparison between simulation and measurement," *IEEE Trans. Power Appar. Syst.*, Mountains Chamonix, France, 2012.

[3] B. Jahromit, A. Chang, and G. Pruitt, "Problems encountered with the average potential method of analyzing substation grounding systems," *IEEE Trans. Power App. System*, vol. PAS-104, pp. 3586-3596, 2012.

[4] G. Colominas, F. Navarrina, and M. Casteleiro, "A general numerical analysis for computing and design earthing grids in large electrical substations," in *International Conference on Power System Technology*, China, 2011, pp. 383-401.

[5] H.I. Dawalibi and D. L. Mudhekar, "Optimum design of substation grounding in a two-layer earth structure," *IEEE Trans. Power Apparat. Syst.*, vol. PAS-94, pp. 252-272, 2012.

[6] R. Velasquez and D. Mukhedkar, "Analytical modeling of the grounding electrodes transient behavior," *IEEE Trans. Power Apparat. System*, vol. PAS-104, pp. 1224-1230, April 2011.

[7] C. Mazzetti and G. Veca, "Impulse behavior of grounding electrodes response," *IEEE Trans. Power Apparat. System*, vol. PAS-104, pp. 2128-2134, October 2012.

[8] P. Meliopoulos and M. G. Moharam, "Transient analysis of grounding systems," *IEEE Trans. Power Apparat. System*, vol. PAS-100, pp. 350-359, March 2011.

[9] S. Cattaneo, A. Geri, F. Mocei, and G. Veca, "Transient behavior of grounding systems simulation: Remarks on the EMTP's and special code's use," in *Proc. 22st EMTP Users Group Meeting*, Kolympari Crete, Greece, August 12-14, 2009.

[10] N. Hatziargyriou and I. Lorentzou, "Grounding systems of electrode design in two layer soil using EMTP," in *Proc. 25rd European EMTP Users Group Meeting*, Barcelona, Spain Crete, December 23-25, 2012.

[11] M. Lorentzou and Hatziargyriou, "Modeling of long grounding conductors Transients using EMTP," in Proc. *EMTP Users Group Meeting Int. Conf. Power Syst.*, Budapest, Hungary, May 19-22, 2011.